Surface Characteristics of Nanocrystalline Apatites: Effect of Mg Surface Enrichment on Morphology, Surface Hydration Species, and Cationic Environments

Luca Bertinetti, Christophe Drouet, Christèle Combes, Christian Rey, Anna Tampieri, Salvatore Coluccia, Gianmario Martra

Surface Characteristics of Nanocrystalline Apatites: Effect of Mg Surface Enrichment on Morphology, Surface Hydration Species, and Cationic Environments

Luca Bertinetti, Christophe Drouet, Christele Combes, Christian Rey, Anna Tampieri, Salvatore Coluccia, and Gianmario Martra

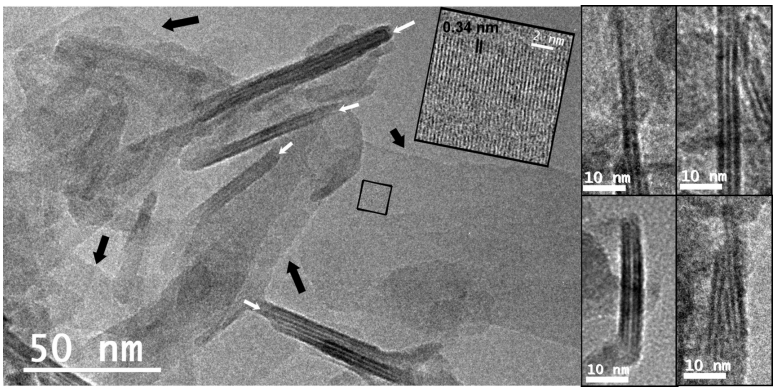

Surface Characteristics of Nanocrystalline Apatites: Effect of Mg Surface Enrichment on Morphology, Surface Hydration Species, and Cationic Environments

Luca Bertinetti,*[,†] Christophe Drouet,[‡] Christele Combes,[‡] Christian Rey,[‡] Anna Tampieri,[§] Salvatore Coluccia,[†] and Gianmario Martra[†]

[†]*Dipartimento di Chimica IFM e NIS Center of Excellence, Università degli studi di Torino, V. Giuria 7, 10125 Torino, Italy ,* [‡]*CIRIMAT Carnot Institute, Université de Toulouse, CNRS/INPT/UPS, ENSIACET, 118 route de Narbonne, 31077 Toulouse Cedex 4, France and* [§]*ISTEC - CNR, V. Granarolo 64, 48018 Faenza, Italy*

The incorporation of foreign ions, such as Mg^{2+}, exhibiting a biological activity for bone regeneration is presently considered as a promising route for increasing the bioactivity of bone-engineering scaffolds. In this work, the morphology, structure, and surface hydration of biomimetic nanocrystalline apatites were investigated before and after surface exchange with such Mg^{2+} ions, by combining chemical alterations (ion exchange, H_2O-D_2O exchanges) and physical examinations (Fourier transform infrared spectroscopy (FTIR) and high-resolution transmission electron microscopy (HRTEM)). HRTEM data suggested that the Mg^{2+}/Ca^{2+} exchange process did not affect the morphology and surface topology of the apatite nanocrystals significantly, while a new phase, likely a hydrated calcium and/or magnesium phosphate, was formed in small amount for high Mg concentrations. Near-infrared (NIR) and medium-infrared (MIR) spectroscopies indicated that the samples enriched with Mg^{2+} were found to retain more water at their surface than the Mg-free sample, both at the level of H_2O coordinated to cations and adsorbed in the form of multilayers. Additionally, the H-bonding network in defective subsurface layers was also noticeably modified, indicating that the Mg^{2+}/Ca^{2+} exchange involved was not limited to the surface. This work is intended to widen the present knowledge on Mg-enriched calcium phosphate-based bioactive materials intended for bone repair applications.

1. Introduction

Nanocrystalline apatites, whether biological (bone mineral, calcifications) or synthetic, exhibit an extended surface area linked to the nanometre size of their constitutive crystals.[1] Because of the high surface-to-volume ratio, all experimental results are thus a combination of bulk and surface contributions. The importance of surface behavior is especially crucial for biomedical applications since numerous functions of the bone mineral occur at the interface between the surface of such apatite nanocrystals and the surrounding biological fluids.

Previous results based on spectroscopic studies, including Fourier transform infrared (FTIR) and solid-state NMR, revealed the existence of nonapatitic chemical environments for ions located on the surface of apatite nanocrystals (biological or synthetic)[2−4] highly sensitive to surface ion exchange processes.[5] Part of these ionic environments were shown to be in strong interaction with hydrated domains,[6,7] leading to the concept of a structured nonapatitic "hydrated layer" present on the surface of apatite nanocrystals and containing relatively mobile ions (mainly bivalent anions and cations).[8]

This layer is thought to be responsible for most of the properties of apatites, and can, for example, help to explain the regulation by biological apatites of the concentration in mineral ions in body fluids (homeostasis) and the fact that bone mineral is an "ion reservoir"[9] capable of releasing or fixing several types of ions.[10,11] However, the exact structure of this layer is still under investigation. Magnesium in bone and biomimetic synthetic samples is considered to belong to the surface of crystals, and it has been shown to alter the morphology and growth rate of crystals.[12]

Also, the postenrichment (with biologically active ions such as magnesium) of synthetic three-dimensional scaffolds intended for bone repair is increasingly considered in the biomaterials field in view of activating the bone regeneration process.[13]

*Corresponding author. Fax: +39 0116706351. Tel: +39 0116706343. E-mail: luca.bertinetti@unito.it.

(1) Elliot, J. C. *Structure and Chemistry of the Apatites and Other Calcium Orthophosphates*; Elsevier: Amsterdam, **1994**.

(2) Rey, C.; Lian, J.; Grynpas, M.; Shapiro, F.; Zylberberg, L.; Glimcher, M. J. *Connect. Tissue Res.* **1989**, *21*, 267–273.

(3) Rey, C.; Strawich, E.; Glimcher, M. J. In *Bulletin Oceanographique*; Allemand, D., Cuif, J. P., Eds.; Musée Océanographique: Monaco, **1994**; pp 55−64.

(4) Wu, Y.; Ackerman, J. L.; Kim, H. M.; Rey, C.; Barroug, A.; Glimcher, M. J. *J. Bone Miner.Res.* **2002**, *17*, 472–480.

(5) Cazalbou, S.; Eichert, D.; Ranz, X.; Drouet, C.; Combes, C.; Harmand, M. F.; Rey, C. *J. Mater. Sci.: Mater. Med.* **2005**, *16*, 405–409.

(6) Eichert, D.; Sfihi, H.; Combes, C.; Rey, C. *Key Eng. Mater.* **2004**, *254−256*, 927–930.

(7) Jager, C.; Welzel, T.; Meyer-Zaika, W.; Epple, M. *Magn. Reson. Chem.* **2006**, *44*, 573–580.

(8) Eichert, D.; Combes, C.; Drouet, C.; Rey, C. *Key Eng. Mater.* **2005**, *284−286*, 3–6.

(9) Yaszemski, M. J.; Payne, R. G.; Hayes, W. C.; Langer, R.; Mikos, A. G. *Biomaterials* **1996**, *17*, 175–185.

(10) Driessens, F. C. M.; Van Dijk, J. W. E.; Verbeeck, R. M. H. *Bull. Soc. Chim. Belges* **1986**, *95*, 337–342.

(11) Rude, R. K.Magnesium homeostasis. In *Principles of Bone Biology*2nd ed.; Bilezikian, J. P., Raisz, L. G., Rodan, G. A., Eds.; Academic Press: San Diego, **2002**; pp 339−358.

(12) Eanes, E. D.; L.; Rattner, S. *J. Dent. Res.* **1981**, *60*, 1719 –1723.

(13) Drouet, C.; Carayon, M.-T.; Combes, C.; Rey, C. *Mater. Sci. Eng., C* **2008**, *28*, 1544–1550.

DOI: 10.1021/la804230j

Although some literature studies dealt with the interaction between such ions and apatitic materials, the samples considered therein were precipitated in the presence of Mg^{2+} and not prepared by a two-step process involving Ca^{2+}/Mg^{2+} substitutions via surface ion exchanges realized *a posteriori*. Also, biomimetic apatites have been rarely considered, and the presence of an extended hydrated layer on the surface of apatite nanocrystals was generally not analyzed.

The goal of this contribution is to investigate in further details the surface state of biomimetic apatite nanocrystals, exploring the particle morphology and following the interaction between water molecules and the surface of apatite nanocrystals. This study was carried out in the absence and in the presence of magnesium, incorporated by surface exchange with calcium ions, in order to eventually unveil modifications due to the presence of Mg^{2+} ions.

2. Experimental Details

2.1. Materials Synthesis. Biomimetic nanocrystalline apatites were synthesized in this work at ambient temperature and physiological pH by double decomposition between a solution of ammonium hydrogenphosphate (120 g $(NH_4)_2HPO_4$ in 1500 mL) and a solution of calcium nitrate (52.2 g $Ca(NO_3)_2$, $4H_2O$ in 750 mL). The calcium solution was rapidly poured into the phosphate solution at room temperature (r.t.; 20 °C). An excess of phosphate was used so as to maintain a pH buffered around 7.4. The precipitate was either filtered immediately (sample "hap-0d") or allowed to mature in the mother solution for one day (sample "hap-1d") and then vacuum-filtered, washed with deionized water (2 L), freeze-dried, and stored in a freezer (−18 °C) to prevent further alteration. It is known that freeze-drying can alter to some extent the surface characteristics of wet nanocrystalline apatites and nanocrystals.[8] However, these alterations are much less drastic than for usual drying techniques (in conventional drying ovens), and freeze-drying thus appears as the most appropriate way to obtain dry apatite powders while limiting the surface modifications for the nanocrystals. Nevertheless, gel-like immature apatites were also investigated here so as to unveil, in the wet state, the existence of possible alterations of the local chemical environment of phosphate groups upon Mg-enrichment. Such gels were obtained as above, but without freeze-drying the samples, and physicochemical analyses were carried out instantly.

2.2. Ca^{2+}/Mg^{2+} Ion Exchange. Ca^{2+}/Mg^{2+} ion exchange experiments were carried out in solution, at r.t., by contacting for 12 min the apatite samples, either as freeze-dried powders or as gels, in an aqueous solution containing increasing concentrations of magnesium chloride (0.1, 0.5, and 1.0 M). A constant solid/solution ratio was used for all experiments (1 g of apatite in 250 mL of exchange solution). After 12 min, the ion-exchanged apatites were separated by filtration, washed with deionized water, and freeze-dried. Drouet et al.[13] showed that this 12-min period was sufficient to reach a stabilization in the Mg content (without enabling the nanocrystals to mature further in solution), and that this protocol led in a reproducible and reversible way, to an actual Ca^{2+}/Mg^{2+} ion exchange (substitution), as witnessed by the removal of surface Ca^{2+} ions from the apatite sample and the simultaneous substitution of an equal amount of Mg^{2+} ions from the solution, rather than a simple adsorption of some magnesium salt. In the text, the notation "hap-1d X% Mg" denotes an apatite sample, matured during 1 day, and enriched with magnesium by ion exchange, leading to the final Mg content of "X" weight %.

2.3. Characterization. The calcium (or calcium plus magnesium) content of the apatite sample was determined by chemical titration of a complex ion formed by interaction of alkaline earth ions and an excess of ethylenediaminetetraacetic acid (EDTA).[14] The phosphate was titrated by visible spectrophotometry (Hitachi U1100) using a colored phosphovanadomolybdate complex.[14] The Mg content of the samples was determined by atomic absorption (Perkin-Elmer A-Analyst 300) after dissolution in perchloric acid.

The crystal structure of the samples was investigated by powder X-ray diffraction (XRD) using an Inel diffractometer CPS 120 and the CoK_α radiation (λCo = 1.78892 Å).

High-resolution transmission electron microscopy (HRTEM) analyses was performed on a JEOL JEM 3010-UHR, operating at 300 kV. As apatite samples might evolve under the electron beam, potentially leading to further crystallization and/or to a loss of constitutive water,[15−18] observations were carried out under feeble illumination conditions (significantly lower than that indicated in the references) to avoid any modifications of the materials during the analysis.

FTIR spectroscopic analysis was used for general infrared characterization of the apatite samples (powders and gels). Such analyses were carried out on a Perkin-Elmer 1600 spectrometer with a resolution of 4 cm^{-1}, using the KBr pellet method. The study of the surface hydration was also carried out in this work, by IR spectroscopy in the near- (NIR) and mid- (MIR) infrared ranges. The samples were studied in equilibrium with the water vapor pressure, and also after outgassing at r.t. Because of the prevalence of heavy scattering of light, NIR measurements were performed in the diffuse reflectance (DR) mode. The powdered samples were put in cells with an optical quartz window, and the spectra were collected using a Perkin-Elmer Lambda 19 instrument, equipped with an integrating sphere coated with $BaSO_4$ also used for the reference spectrum. Differently, MIR spectra were collected in the transmission mode (Bruker V22, MCT detector, 4 cm-1 resolution) on self-supporting pellets of the materials put in cells equipped with KBr windows. For both NIR and MIR measurements, the cells were permanently connected to conventional high vacuum lines (residual pressure: 1.0×10^{-6} Torr; 1 Torr = 133.33 Pa), allowing desorption and adsorption experiments to be carried out in situ.

H_2O/D_2O isotopic exchange was also performed, by contacting the materials outgassed at r.t. with D_2O vapor. For these experiments, several D_2O admission/outgassing cycles were performed, followed by MIR analyses.

3. Results and Discussion

3.1. Global Characterization and Ca^{2+}/Mg^{2+} Ion Exchanges. Freeze-dried apatite powders obtained after 0 and 1 day of maturation in solution, hap-0d and hap-1d, respectively, were analyzed by XRD (Figure 1). Both samples exhibit the apatite structure, although the width of the diffraction lines indicates a rather low degree of crystallinity, fully comparable to that of bone mineral.[1] Also, an increase in degree of crystallinity can be remarked after a day of maturation. Chemical analyses performed on both samples led to Ca/P ratios in the range 1.40−1.46 (Table 1), pointing out the nonstoichiometry of apatites prepared by this double decomposition route (the Ca/P ratio for stoichiometric hydroxyapatite being 1.67). The evaluation of the average crystallite size by Scherrer's formula applied to diffraction lines (002) and (310), respectively giving information along

(14) Charlot, G. *L'analyse Quantitative*; Masson: Paris, **1956**.
(15) Meldrum, A.; Wang, L. M.; Ewing, R. C. *Am. Mineral.* **1997**, *82*, 858–869.
(16) Celotti, G.; Tampieri, A.; Sprio, S.; Landi, E.; Bertinetti, L.; Martra, G.; Ducati, C. *J. Mater. Sci.: Mater. Med.* **2006**, *17*, 1079–1087.
(17) Vallet-Regi, M.; Gutierrezrios, M. T.; Alonso, M. P.; Defrutos, M. I.; Nicolopoulos, S. *J. Solid State Chem.* **1994**, *112*, 58–64.
(18) Wang, L. M.; Wang, S. X.; Ewing, R. C.; Meldrum, A.; Birtcher, R. C.; Provencio, P. N.; Weber, W. J.; Matzke, H. *Mater. Sci. Eng., A* **2000**, *286*, 72–80.

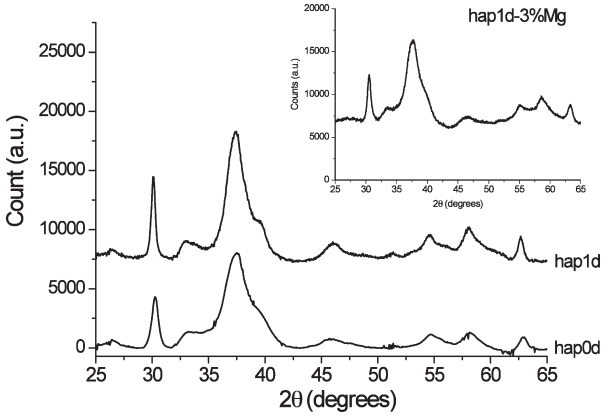

Figure 1. XRD patterns of hap-0d and hap-1d. Inset: XRD pattern obtained on hap-1d after Mg/Ca exchange.

the *c*-axis of the structure and in a perpendicular direction, showed the nanometre scale dimensions of the constitutive apatite crystals (Table 1). The longer crystallite dimension observed along the *c*-axis is a usual finding and is due to the platelet shape of such nanocrystalline apatites (biological as well as synthetic analogues), departing from the theoretical hexagonal apatitic system.

The magnesium uptake by apatite crystals after Ca^{2+}/Mg^{2+} ion exchange at concentrations in the exchange solution of 0.1, 0.5, and 1.0 M was investigated. Such exchange experiments were first attempted on both hap-0d and hap-1d samples. However, the tests performed on hap-0d pointed out (especially after XRD analysis) a non-negligible evolution of the nanocrystals during the 12-min exchange period, making further interpretations more delicate. For this reason, the exchange experiments described in the following relate to the sample hap-1d, which is much less sensitive than hap-0d to further maturation during the exchange experiments. The magnesium contents measured by atomic absorption were 0.9, 1.3, and 3.0 wt. %, respectively for the concentrations of 0.1, 0.5, and 1 M in the exchange solution. It is worth noting that XRD analysis of such Mg-enriched apatite is still characteristic of nanocrystalline apatite (see inset in Figure 1), and the presence of secondary crystalline Mg-containing phases was not observed (within the detection limits of the diffractometer). These findings can be compared to those reported in a recent paper,[13] and illustrate the possibility to modify the (surface) Mg content on such apatite nanocrystals, by controlling the powder preparation conditions and by varying the concentration of the exchange solution.

The study by FTIR spectroscopy of apatite samples before and after Ca^{2+}/Mg^{2+} ion exchange can also be of great interest in order to follow potential alterations of ionic chemical environments. However, such an FTIR analysis is only moderately informative for freeze-dried matured samples compared to wet immature ones since the extent of their hydrated layer is limited by the maturation and modified by the freeze-drying step.[5−8] In this context, the analysis of apatites that have not been matured and are still in their wet state (exhibiting a gel-like appearance) is potentially much more informative because of their more extended and unaltered hydrated layer (even though TEM observations are not possible on such wet samples).

In this view, freshly precipitated apatite gels were prepared and analyzed by FTIR spectroscopy. The IR spectra related to Mg-free gels were found to exhibit a fine structuration

Table 1. Ca/P Ratio and Average Crystallite Size for Samples hap-0d and hap-1d

sample	hap-0d	hap-1d
Ca/P (mol)	1.40	1.46
Estimated Crystallite Size (Scherrer's Formula)		
(002)	16 nm	26 nm
(310)	5 nm	6 nm

(adjacent thin bands), especially in the range 900−1200 cm^{-1}, characteristic of the $\nu_1\nu_3(PO_4)$ region (Figure 2, "Mg-free apatite gel"), which was previously linked[6] to the existence of a structured hydrated layer with characteristics close, although not identical, to those of octacalcium phosphate (OCP, as shown in Figure 2). It therefore reveals a strong alteration of phosphate chemical environments in the presence of magnesium. Interestingly, this effect was found to be mostly reversible for wet apatite samples, as a spectrum close to the original one can be observed again after reverse exchange of Mg^{2+} ions with Ca^{2+} (performed by soaking the Mg-exchanged powder in a calcium 1.0 M solution). This analysis on apatite gels reveals that Ca^{2+}/Mg^{2+} cationic exchange can lead to strong modifications of (at least) phosphate ionic environments in the hydrated layer of such apatite-based materials.

3.2. Morphology and Structure of Materials. TEM observations of the Mg-free sample hap-1d showed that it is composed of particles elongated in one direction, with length and width (in the bidimensional projection on the image plane) in the 25−100 nm and 10−30 nm range, respectively, and exhibiting rounded edges (Figure 3a). Unfortunately, no particles appeared oriented with a zone-axis parallel to the electron beam, and this prevented the possibility to observe crossing diffraction fringes, the simulation of which can make allowance to estimate the particle thickness.[19] The observed dimensions are significantly larger than the size of the crystalline domains estimated from the XRD data (Table 1), pointing out for the polycrystalline nature of the particles after freeze-drying.

At high magnification, some series of diffraction fringes were detected for several particles. An example is shown in Figure 3b, where a regular pattern with separation of 3.41 Å, oriented perpendicularly to the elongation direction of the particle, can be observed. As the fringe spacing corresponds to that of (002) planes of the hydroxyapatite lattice, it can be concluded that the particle is elongated along the *c*-axis of the hexagonal structure. Interestingly, the diffraction fringes, which monitor the presence of a crystalline structure, were extended almost up to the surfaces of the particle, but the borders appeared quite irregular, indicating that no specific crystalline planes were actually exposed at the surface of the particles. These observations are of prime importance, as they are a direct observation and are in agreement with the existence of a nonapatitic hydrated layer on the surface of the apatite nanocrystals constituting such particles, as was discussed in detail previously.[3,5] The alteration of the samples under the electron beam at even higher magnifications prevented the possibility to obtain more detailed images of the borders, and then of the actual thickness of this surface disordered region. However, it should be thinner than 2 nm, because amorphous surface

(19) Williams, D. B.; Carter, C. B. *Transmission Electron Microscopy: A Textbook for Materials Science*; Plenum Publishing: New York, **1996**; Vol. *3*.

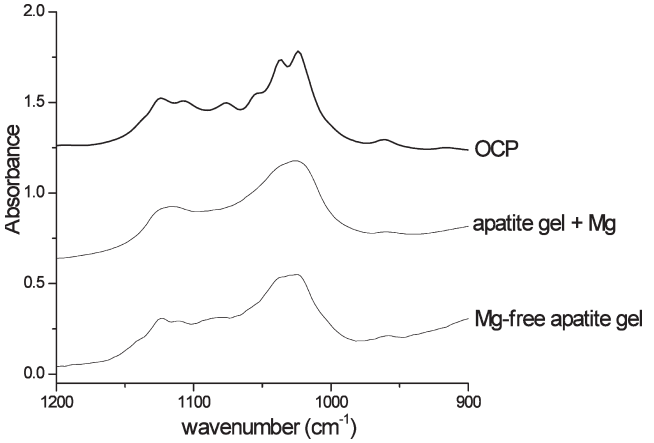

Figure 2. FTIR analysis for $\nu_1\nu_3(PO_4)$ vibration mode for immature apatite gel before and after Mg-surface enrichment by ion exchange, and for OCP.

layers of such extension were already observed for other apatitic materials in similar conditions.[20]

In the case of the samples that underwent the Mg^{2+}/Ca^{2+} exchange, essentially the same type of results were obtained in all cases; therefore, only an image of hap-1d 0.9% Mg is shown in Figure 4 as a representative of the set of three samples. A significant fraction of the particles were found to retain the sizes observed for hap-1d (e.g., particles indicated with a black arrow in Figure 4), with width and length in the 10−50 nm and 30−100 nm range, respectively, with the main dimension being along the *c*-axis, as derived from the analysis of images taken at higher magnification (inset of Figure 4A).

It is worth noting that, after Mg enrichment, a detectable amount of particles (evidenced by white arrows in Figure 4A) exhibiting different dimensional features, i.e., a quite small width (3−10 nm) and an important length (up to 200 nm) were observed. Although these particles remained in low proportion, their amount was found to increase with the Mg content of the samples. These particles appeared to be characterized by some degree of structural order, as indicated by a set of fringes running parallel to their length. However, the measured interplanar spacings were not constant and varied from 0.9 to 1.6 nm, not only depending on the particle considered, but even inside a given particle (Figure 4 B−E). As the special frequency of these fringes is very low, they can be directly related to the structure of the material itself.[21] In particular, black fringes and white fringes should correspond to atomically denser and less dense planes, respectively, and most of these secondary particles appeared to be constituted by 2, 3, or 4 planes.

Because the measured interfringes spacing varied in a quite wide range, it has not been possible so far to unequivocally identify a mineral phase these particles can belong to. However, they are not compatible with a hydroxyapatite phase, whereas some similarities can be found with hydrated magnesium and/or calcium−magnesium phosphates; it can be hypothesized that such secondary particles might result from

(20) Bertinetti, L.; Tampieri, A.; Landi, E.; Ducati, C.; Midgley, P. A.; Coluccia, S.; Martra, G. *J. Phys. Chem. C* **2007**, *111*, 4027–4035.

(21) Such a statement was based on the consideration that the transfer function of the microscope did not change in sign for the range of defocus values used to acquire the images.

(22) Lher, J. R.; Brown, E. H.; Frazier, A. W.; Smith, J. P.; Thrasher, R. D. *NFDC Bull.* **1967**, *6*, 46–47.

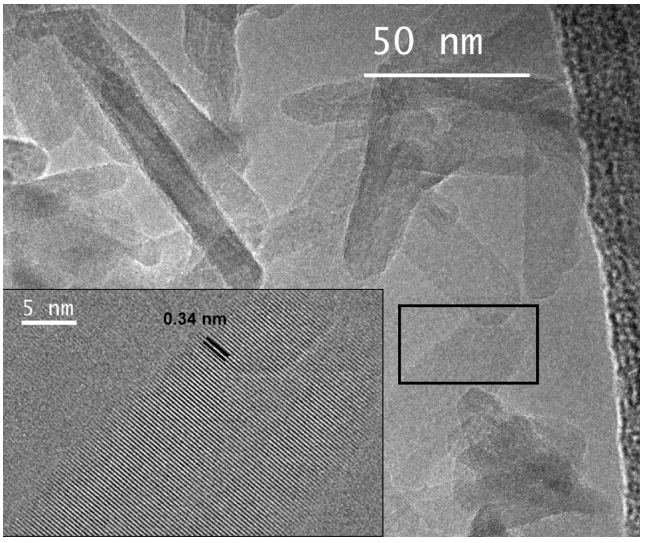

Figure 3. TEM micrograph of hap-1d. Main panel: low-magnification image of apatite particles (original magnification: 80K×); inset: high-resolution image of the enframed region in the main panel (original magnification: 300K×).

an incipient formation of a phase such as hydrated calcium and/or magnesium phosphates,[22] with the thickness of both atomically dense layers (dark fringes in the electron micrographs) and hydration regions (bright fringes in the electron micrographs) changing from particle to particle and from plane to plane.

The difficulty for magnesium to be incorporated in the apatite structure as well as the high amount of water molecules can probably account for the formation of a hydrated Mg-containing phase for samples with high Mg contents. It was, however, very difficult to estimate the relative amount of this second family of particles with respect to the primary apatitic particles because of their extremely light contrast when separated (even partially) one from the other, and also because, in most cases, particles were gathered in aggregates too thick to allow the observation of the contour of single components. Nevertheless, it must be considered that this phase escaped the detection by XRD, as no diffraction peaks were detected in the angular range corresponding to the measured spacing. Although the irregularity in the structure of such particles could partly account for a decreased capability to contribute to a XRD pattern, it can be assessed that the new phase could reach a few percents in volume of the samples, in particular after an exchange procedure with samples exhibiting a high Mg content.

3.3. Effect of Ca^{2+}/Mg^{2+} Exchange on Surface Hydration. *3.3.1. Preliminary Remarks.* As indicated in the Introduction, an additional goal of this study was to investigate the effect of the Ca^{2+}/Mg^{2+} exchange on the surface hydration state of the sample, which in turn should be related to changes in the nature and structure of surface sites. The samples were studied when in equilibrium with the water vapor pressure, and also after a subsequent outgassing at r.t. By switching between these two conditions, the surface hydration was decreased from the presence of multiadlayers of water to that of a single layer made of H_2O molecules left adsorbed on the surface as being involved in a coordinative interaction with cationic centers and H-bonding with phosphate groups, respectively.[20] In previous studies on Ca^{2+} and Ca^{2+}/Mg^{2+} nanocrystalline hydroxyapatites produced by different protocols, we demonstrated that it was possible

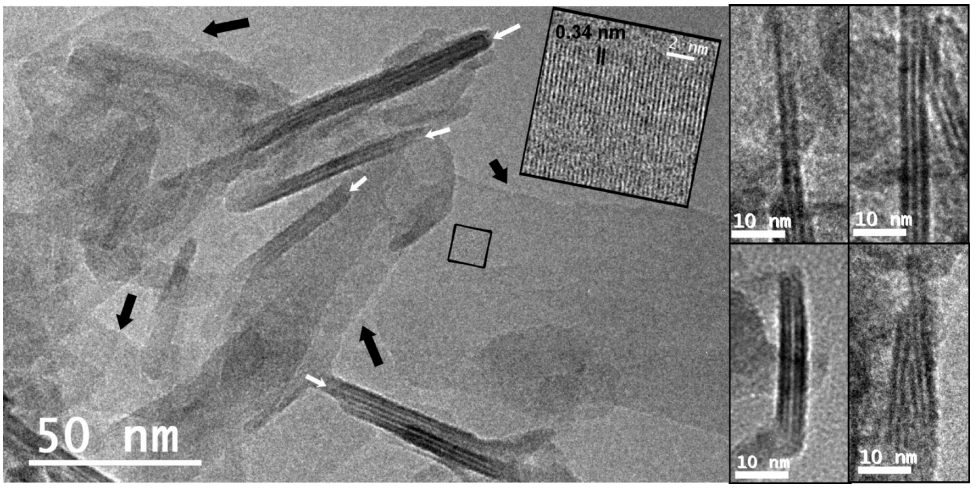

Figure 4. TEM micrographs of hap-1d 0.9% Mg. (A) Mainframe: low-magnification image of the material (original magnification: 80K×); black arrows indicate particles similar to those observed for the parent hap-1d material; white arrows indicate new phase particles; Inset: magnified view of the enframed region of an apatitic particle. (B−E) Magnified view of new phase particles constituted by 2, 3, and 4 planes (B−D, in that order), and exhibiting structural defects (E).

to obtain insight into surface cationic centers by IR spectroscopy of adsorbed probe molecules, namely CO.[20,23] However, the adopted procedures implied the removal of H_2O molecules initially adsorbed on such sites, and this was obtained by outgassing the material above r.t. Unfortunately, the biomimetic samples studied in the present work are, like biological apatites, extremely sensitive to outgassing treatments, which leads to an extensive modification of the surface structure, as monitored by the significantly lower amount of water that the materials were able to readsorb subsequently (not shown for the sake of brevity). As a consequence, the investigation of the relative amount and local structure of surface sites hosting Ca^{2+} or Mg^{2+} ions was not possible.

3.3.2. NIR Studies. To reach a standard condition representative of the adsorption capability toward water, the samples were outgassed at room temperature and then equilibrated with the H_2O vapor pressure (ca. 24 mbar) at r.t. Because of the high specific surface area, the number of H_2O molecules adsorbed in the presence of water vapor was so high that their typical absorption bands in the MIR region (due to stretching and deformation modes) exceeded the maximum of the absorbance scale. However, such a limitation did not occur for absorption bands in the NIR region, where overtones and combination transitions[24] absorb with much weaker extinction coefficients. Water NIR signals in the 6800−7200 cm^{-1} range appeared partially overlapped by the 2ν(OH) overtone signals related to silanol defects in the optical quartz of the cell used for the DR measurements and to OH^- in the bulk of the materials studied (not shown for the sake of brevity). For this reason, attention was focused on the band due to the H_2O $\delta + \nu_{asym}$ combination mode,[25] located in the 5500−4500 cm^{-1} range. Such a mode was found to be quite sensitive to the number and strength of hydrogen bonds the water molecules can be involved in. As a consequence, the corresponding NIR absorption band contains several components, each related to ensembles of molecules experiencing a different set of interactions.[24,26]

The analysis of the $\delta + \nu_{asym}$ H_2O band observed for the sample hap-1d (Figure 5A, a) shows that it is composed of several components, with a main band located at ca. 5170 cm^{-1} that can be attributed to H_2O molecules acting as a donor of two equivalent H-bonds, and two shoulders at ca. 5300 (narrower) and ca. 5000 (broader) cm^{-1}, likely due to the OH moieties (non H-bonded and H-bonded, respectively) of water molecules acting as a donor of a single H-bond.[24] Similar features were observed by Ishikawa et al., in their study on colloidal nonstoichiometric hydroxyapatite.[27] The introduction of Mg^{2+} at both 0.9 and 1.3 wt % levels resulted in a similar, slight increase of the overall intensity of the $\delta + \nu_{asym}$ H_2O band, particularly noticeable for the shoulders at ca. 5300 and 5000 cm^{-1} (Figure 5A, b,c). Differently, in the case of hap-1d 3.0% Mg, the $\delta + \nu_{asym}$ H_2O signal appeared significantly more intense and less structured, because of the presence of a main component at ca. 5120 cm^{-1}, assignable to H_2O molecules involved as donors of two equivalent H-bonds (Figure 5A, d).

The next step of the investigation was focused on the states of water molecules left adsorbed on the surface after outgassing at r.t. The actual location of such H_2O molecules on the surface only, and not entrapped in the bulk, was assessed by H_2O/D_2O exchange, which resulted in the depletion of the signals due to water in favor of downshifted components due to D_2O (not shown for the sake of brevity; an analogous behavior observed in the MIR region is reported in the following). Focusing on the spectra of H_2O irreversibly adsorbed at r.t., besides an obvious significantly lower intensity, the $\delta + \nu_{asym}$ pattern obtained for the hap-1d sample exhibited two components partially overlapped: one at ca. 5190 cm^{-1} and the other, quite broader, centered at ca. 4950 cm^{-1} (Figure 5B, a). In the case of samples enriched with Mg^{2+}, an additional broad component spread

(23) Bertinetti, L.; Tampieri, A.; Landi, E.; Martra, G.; Coluccia, S. *J. Eur. Ceram. Soc*. **2006**, *26*, 987–991.

(24) Burneau, A.; Barres, O.; Gallas, J. P.; Lavalley, J. C. *Langmuir* **1990**, *6*, 1364–1372.

(25) Insofar as a water molecule is symmetrical in a condensed state, the stretching modes with the lowest and the highest wavenumber, usually indicated as $\nu 1$ and $\nu 3$, correspond to its symmetrical and antisymmetrical stretching vibration, respectively. In the case of removal of the symmetry of water molecules by interaction with neighbour species, the notations ν_{sym} and ν_{asym} indicate the in phase and out-of-phase hydroxyls stretching, respectively.

(26) Takeuchi, M.; Bertinetti, L.; Martra, G.; Coluccia, S.; Anpo, M. *Appl. Catal. A: Gen*. **2006**, *307*, 13–20.

(27) Ishikawa, T.; Wakamura, M.; Kondo, S. *Langmuir* **1989**, *5*, 140–144.

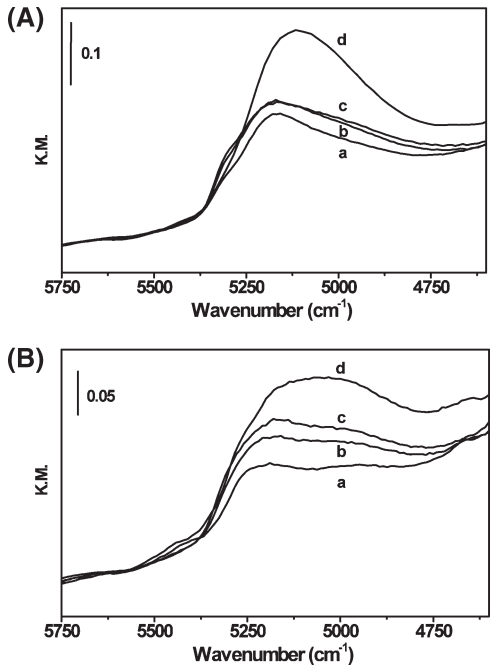

Figure 5. NIR spectra in the 5750−4720 cm^{-1} range of hap-1d (a), hap-1d 0.9% Mg (b), hap-1d 1.3% Mg (c), and hap-1d 3.0% Mg (d). Panel A: in contact with water vapor pressure; panel B: after outgassing at room temperature for 1 h.

over the 5150−5000 cm^{-1} range appeared, and the intensity of the overall pattern similarly increased for both hap-1d 0.9% Mg and hap-1d 1.3% Mg (Figure 5B, b,c), while the intensity gain was much higher for hap-1d 3.0% Mg (Figure 5B, d).

Of particular interest is the absence of any high-frequency component possibly related to water molecules acting as donors of only one H-bonding, indicating that the adsorbed H_2O molecules have both O−H involved in hydrogen bonds, in agreement with the results of simulation studies.[28−30] Unfortunately, the broadness and overlapping of the various component prevented (at least at present) a more detailed assignment. It can, however, be stated that the lower the frequency of a $\delta + \nu_{asym}$ component, the stronger the H-bonding (resulting in a downshift of the ν_{asym} contribution) and/or the stronger the coordination to a surface site through the O atom (resulting in a downshift of the δ contribution) of H_2O molecules responsible for that signal.

In summary, for Ca^{2+}/Mg^{2+} exchange, the surface hydration of the materials appeared to be modified in terms of (i) structure of the adsorbed water (changes in the relative intensity and position of the components), and (ii) increase of the capability to adsorb water.[31] Interestingly, these modifications are not limited to water molecules in direct contact with the surface (Figure 5B), but are extended to water overlayers (Figure 5A).

Although a punctual description of surface sites was not possible (see above), it is reasonable to propose that at least a relevant part of such modifications of the surface hydration may result from the presence at the surface of Mg^{2+} ions, which are known to interact more strongly with H_2O molecules than Ca^{2+}.[32]

Actually, the increase of the amount of adsorbed water did not appear to be linearly proportional to the Mg^{2+} content. Confirmatory insights were provided by the following steps of the IR study.

3.3.3. MIR Study; H/D Exchange by Contact with D_2O. Because of the lower amount of adsorbed H_2O, the intensity of the bands in the MIR range exhibited by the materials outgassed at r.t. is much lower; therefore, the transmission spectra in such region could be collected. The spectral patterns obtained for the various samples (Figure 6) were characterized by a quite weak, narrow peak at 3567 cm^{-1}, due to bulk OH− in regular apatitic lattice positions,[33] while the very broadband spread over the 3750−2250 cm^{-1} range should result from the overlapping of components related to the ν(OH) modes of H-bonded hydroxy groups (likely related to O−H vibrations in HPO_4 groups). The minor features around 2000 cm^{-1} are due to overtones and combination modes of bulk phosphates,[33] followed at lower frequency by the $\delta(H_2O)$ band (1700−1550 cm^{-1} range). At further lower frequency, weak bands due to some carbonate group were present; therefore, the material appeared totally opaque, because of the complete absorption of the IR radiations by the bulk phosphate fundamental modes. At the best of our knowledge, the only feature not described and/or assigned on in the IR studies of hydroxyapatite reported in the literature is the minor component at ca. 2500 cm^{-1}.

A detailed discussion of the nature of such component is out of the scope of this paper, but it can tentatively be assigned to a Fermi resonance effect between the ν(OH) mode of P-OHs moieties, downshifted by a strong H-bonding, and the overtone of the δ(POH) mode occurring at lower frequency (likely below the transparency cutoff of the samples), as observed for S-OH groups in Nafion membranes.[34] The Fermi resonance is expected to produce a doublet, but in the present case the partner of the 2500 cm^{-1} feature could be confused in one of the broad absorptions on the high or low frequency side of this latter.

Among the spectral components due to water molecules, the one related to their δ mode was the most clearly observable because it did not overlap with other signals, and an enlarged view of the $\delta(H_2O)$ band observed for the four materials is depicted in the inset of Figure 6. In agreement with the trend observed for the NIR spectra, the integrated intensity of this band increased when passing from the parent hap-1d (curve a, with maximum at 1640 cm^{-1}) to the samples containing increasing amounts of Mg^{2+} (curves b−d), essentially because of the growth of a subband at lower frequency, appearing as the dominant component for hap-1d 3.0 wt % Mg, with maximum at ca. 1620 cm^{-1} (curve d). Such a downshift can be considered as the marker of the interaction of H_2O molecules with adsorbing sites with a higher polarizing power than Ca^{2+}, such as Mg^{2+}.[35]

(28) Pareek, A.; Torrelles, X.; Angermund, K.; Rius, J.; Magdans, U.; Gies, H. *Langmuir* **2008**, *24*, 2459–2464.
(29) Pareek, A.; Torrelles, X.; Rius, J.; Magdans, U.; Gies, H. *Phys. Rev. B* **2007**, *75*, 035418.
(30) Mkhonto, D.; de Leeuw, N. H. *J. Mater. Chem.* **2002**, *12*, 2633–2642.
(31) Bolis, V.; Fubini, B.; Marchese, L.; Martra, G.; Costa, D. J. *Chem. Soc., Faraday Trans.* **1991**, *87*, 497–505.
(32) Wilkinson, G. *Comprehensive Coordination Chemistry*; Pergamon Press: Oxford, **1987**; p 3.
(33) Koutsopoulos, S. *J. Biomed. Mater. Res.* **2002**, *62*, 600–612.
(34) Buzzoni, R.; Bordiga, S.; Ricchiardi, G.; Spoto, G.; Zecchina, A. *J. Phys. Chem.* **1995**, *99*, 11937–11951.
(35) Nakamoto, K. *Infrared Spectra of Inorganic and Coordination Compounds*; Wiley Interscience: New York, **1970**; p 167.

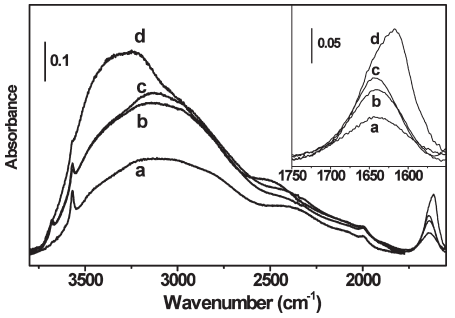

Figure 6. IR spectra of the samples hap-1d (a), hap-1d 0.9% Mg (b), hap-1d 1.3% Mg (c), and hap-1d 3.0% Mg (d) outgassed at r.t. for 1 h.

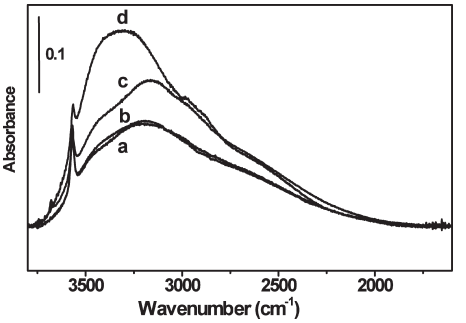

Figure 7. IR spectra of the samples hap-1d (a), hap-1d 0.9% Mg (b), hap-1d 1.3% Mg (c), and hap-1d 3.0% Mg (d) after H_2O/D_2O exchange was complete (after $\nu(D_2O)$ subtraction). The asterisk indicates the position of the band (δ mode) expected in the case of the presence of H_2O molecules).

The analysis of the water stretching bands is more complex, because of their possible superimposition with the signal due to surface/subsurface (vide infra) hydroxy groups, namely, OH^- ions and/or hydroxylated phosphate ions. However, it can be observed that the broad absorption spread over the 3750−2250 cm^{-1} range exhibited a similar increase in intensity when passing from the parent hap-1d (Figure 6, a) to hap-1d 0.9% Mg and hap-1d 1.3% Mg (Figure 6, b,c). In the case of hap-1d 3.0% Mg, the further increase in intensity is essentially due to the appearance of an additional component on the high frequency side (Figure 6, d). The upshifted position of such component indicates that additional H_2O molecules adsorbed on this material interact with the surface, on the one hand, via a stronger coordinative interaction (see above), but, on the other hand, via weaker H-bondings. The combination of two such features could then be responsible for the location of the corresponding $\delta + \nu_{asym}$ NIR band between the components observed for the hap-1d parent sample (see Figure 5B and related comments).

According to the corresponding NIR spectra (Figure 5B), the increase in intensity exhibited by both the stretching and bending bands did not appear strictly proportional to the Mg^{2+} content. This behavior could be due in part to the development of a foreign Mg-rich phase in samples with a high magnesium content; however, if we admit that such a phase represents a very limited amount of the magnesium, it implies that Mg ions of the apatite nanocrystals exhibit different water-binding capabilities. It can be suggested that only part of Mg^{2+} ions might be exposed on the surface, with the remaining Mg^{2+} ions being located in subsurface positions; the ratio between these two fractions depend on the total Mg^{2+} content. It could also be linked, to some extent, to the fact that several sites, with different coordinated water shells, coexist on the surface.

An indirect indication of the occurrence of a modification of subsurface layers as a consequence of the Ca^{2+}/Mg^{2+} exchange was provided by contacting the materials, outgassed at r.t., with D_2O vapor. By this method it was possible to distinguish the IR features due to surface hydration species from those related to hydroxy groups and water molecules (if any) within the particles. Three D_2O admission/outgassing cycles were performed before reaching an invariance of the IR spectra, witnessing the completeness of the isotopic exchange, and the data ultimately obtained are shown in Figure 7.

For the sake of clarity, the signals due to ν(OD) modes (originally in the 2500−2000 cm^{-1} range, see Figure 1 in Supporting Information) were subtracted, while the $\delta(D_2O)$ fell in the nontransparent region of the samples. The absence of any trace of the $\delta(H_2O)$ band indicated that all water molecules were exchanged; therefore, all features still present in the ν(OH) absorption range should be attributed to hydroxyl/hydroxylated groups within the particles. The narrow peak due to OH^- in ordered apatitic positions is among them, but the main signal appeared to be a broad absorption spread over the 3700−2250 cm^{-1} that should be assigned to H-bonded hydroxy groups, likely belonging to HPO_4 groups. Independently of the exact nature of this band, it must be noticed that it exhibited a progressively higher intensity and an overall shift toward higher wavenumbers with increasing Mg^{2+} contents (Figure 7) as compared to the Mg-free sample. Such an evolution suggests that some modification of the subsurface layers should also have occurred during the exchange procedure, with a possible insertion of some Mg^{2+} ions in those layers. These findings can be linked to the results observed by FTIR on immature apatite gels, pointing out the strong disordering effect of Mg^{2+} on the surface ionic arrangement that was especially noticeable around phosphate groups (Figure 2).

4. Conclusions

This contribution deals with the surface characteristics and surface hydration of biomimetic nanocrystalline apatites, before and after surface exchange with magnesium ions, one of the constituents of bone mineral.

The adopted double decomposition method resulted in the production of nanocrystalline apatite particles, elongated along the *c*-axis, as for the mineral particles present in bone. The crystal order appeared to be extended up to their surface, although no regular faces were found to be exposed as surface terminations. This is a peculiar feature with respect to both apatite crystals larger in size[36,37] and nanosized apatite particles differently produced, characterized by a surface amorphous layer a few nanometers thick.[7,20,38] The data reported in the present work are in agreement with preliminary reports on the presence of a nonapatitic surface layer on such apatite nanocrystals. It can also be noted that HRTEM observations detected the presence of a minor secondary phase, possibly a hydrated magnesium-containing phase, particularly in the case of high Mg contents (e.g., 3 wt % Mg); however, its

(36) Suvorova, E. I.; Buffat, P. A. *J. Microsc. (Oxford, U.K.)* **1999**, *196*, 46–58.
(37) Tamai, M.; Nakamura, M.; Isshiki, T.; Nishio, K.; Endoh, H.; Nakahira, A. *J. Mater. Sci.: Mater. Med.* **2003**, *14*, 617–622.
(38) Isobe, T.; Nakamura, S.; Nemoto, R.; Senna, M.; Sfihi, H. *J. Phys. Chem. B* **2002**, *106*, 5169–5176.

feeble amount strongly suggests that this phase does not intervene to a noticeable level in the overall behavior of the Mg-enriched samples.

The IR study of the surface hydration indicated that the Ca^{2+}/Mg^{2+} exchange resulted in an increase of the amount of water molecules adsorbed on the surface, while the process also affected the"sub-surface layers" to some extent.

This work should prove helpful for the understanding of the interaction between biomimetic apatites and magnesium ions, which are increasingly considered in the biomaterials field, for the postactivation of bone repair scaffolds. Considering the results from this study, the samples matured for 1 day and enriched with up to 1 wt % Mg^{2+} appear as specially attractive systems in view of further investigations on the enrichment with magnesium of bone repair bioactive calcium phosphate scaffolds.

Acknowledgment. The authors are grateful to the Piemonte region (Italy) for financial support (Progetto NANOMAT-ASP, Docup 2000-2006, Linea 2.4a), and to the European Commission for support in the scope of the AUTOBONE program (NMP Program NMP3-CT-2003-505711-1).

Supporting Information Available: Original IR spectra of materials after H_2O/D_2O isotopic exchange cycles. This material is available free of charge via the Internet at http://pubs.acs.org.